

Finite-size Effects on the Thermal Resistivity of ^4He Near the Superfluid Transition

Sergei Jerebets,¹ Yuanming Liu,¹ Fengchuan Liu,¹ and Guenter Ahlers²

¹Jet Propulsion Laboratory, California Institute of Technology, Pasadena, CA 91109, USA
E-mail: jerebets@jpl.nasa.gov

²Department of Physics and iQCD, University of California, Santa Barbara, CA 93106, USA
E-mail: guenter@physics.ucsb.edu

We present measurements of the thermal resistivity $\rho(t, L)$ ($t \equiv T/T_\lambda - 1$) near the superfluid transition temperature T_λ of ^4He at saturated vapor pressure and confined in glass capillary arrays with rectangular cross-sections of spacing $L = 1 \mu\text{m}$, width $w = 10 \mu\text{m}$, and length $d \simeq 1 \text{ mm}$. We expect the finite-size effect in this rectangular geometry to provide a good approximation to that in the ideal parallel-plate geometry. The data coincide within our resolution with previous measurements for cylindrical capillaries of $1 \mu\text{m}$ radius, indicating that the finite-size scaling-functions for these two geometries are indistinguishable. This stands in contrast to the scaling functions for static properties which, near the transition temperature, depend on the dimensionality of the confinement. The results are consistent with recent Monte Carlo and spin-dynamics simulations, and with renormalization-group calculations for capillaries with square cross section and $t \geq 0$.

1. INTRODUCTION

The modern theory of critical phenomena¹ predicts that continuous phase transitions of infinitely extended samples belong to distinct universality classes that are determined by such general properties of the system as the number of degrees of freedom of the order parameter and the spatial dimensionality. Within a given universality class, the dependence of many properties upon certain parameters can be represented by scaling functions that are the same for all systems in a given class. The behavior of finite samples is more complex.²⁻⁶ Although for most confinement geometries there is no phase transition, one supposes that the properties may still be described by “universal” scaling functions⁷ even though the transition is “rounded.” Even within a given universality class for the bulk system there may be several sub-classes for samples of finite extent,

depending on the symmetry of the confinement. Thus, for instance it has been shown experimentally that the scaling function for the specific heat of liquid helium near the lambda-point and confined between parallel plates differs from the one for confinement in capillaries with a square cross section or in small cubes.⁸

The present paper is an experimental study of the effect of confinement by a parallel-plate geometry with spacing L , width $w \gg L$, and length $d \gg w$ on a transport property, namely on the thermal resistivity $\rho(t, L)$ of liquid helium near the superfluid transition at T_λ ($t \equiv T/T_\lambda - 1$). For transport properties the possible universality classes can be more diverse because the direction of the current breaks the rotational invariance of the sample. In that case the scaling function can depend both on the dimensionality of the confinement and on the direction of the current relative to the confinement geometry. This is shown in Fig. 1.

For confinement in a cylindrical capillary (Fig. 1(a)) it would seem that the only physically reasonable direction of the current is along the axis of the cylinder. This case was studied experimentally under a number of conditions.⁹⁻¹² However, for the parallel-plate geometry of Fig. 1b and c there are the two distinct cases of a current orthogonal to or in the plane of the sample. With the current orthogonal to the plane and a sufficiently large spacing L , the problem reduces to the interesting one of a boundary resistance¹³⁻²⁰ that has a singularity at the superfluid transition.

Here we focus on the case shown by Fig. 1c where the current is in the plane of the sample. The fluid was confined in glass capillary arrays (GCA) containing capillaries with a rectangular cross section of size $L \times w$ with $L = 1 \mu\text{m}$ and $w = 10 \mu\text{m}$ in the x and y direction, respectively, and of length $d \simeq 1 \text{ mm}$ in the z direction. We expect that the sample is effectively

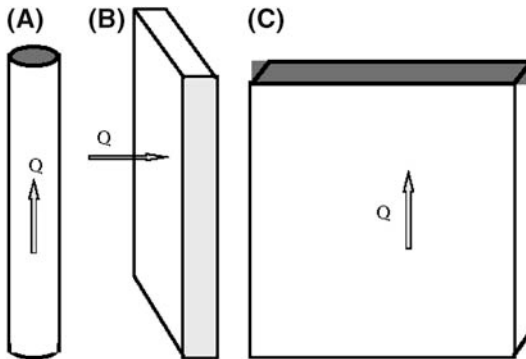


Fig. 1. Illustration of the three possible cases for finite-size effects on transport properties.

Finite-size Effects on the Thermal Resistivity of ^4He

infinite in the z direction and that the size L will impose finite-size effects in the x direction when the absolute value of the reduced temperature $|t|$ is less than some crossover value t_L . The size w in the y direction may warrant some comment. It will also produce finite-size effects in its direction, albeit for $|t| \lesssim t_w$. On the basis of scaling arguments we expect $t_L/t_w \simeq (w/L)^{1/\nu} \simeq 31$ where $\nu \simeq 0.6705$ is the correlation-length exponent.²¹ Since t_w is expected to be much less than t_L , there should be a wide range of the reduced temperature over which the system will exhibit quasi-two-dimensional behavior, thus closely approximating confinement by infinitely extended parallel plates separated by $L = 1 \mu\text{m}$.

A brief comparison with the cylindrical case of cylinder radius r is instructive. In both cases one expects that the geometry effect will become purely a surface effect far enough away from the transition where the correlation length ξ of the order parameter is much smaller than r or L . In that case the deviation from bulk behavior should be proportional to the ratio of the surface area times ξ to the total volume. For the two geometries one readily sees that this is the same when $r = L$. Thus, we expect the resistivities of the cylindrical and the parallel-plate cases to merge as the distance from the phase transition increases when $r = L$. However, as was the case for the thermodynamic properties, the scaling functions need not be the same near the transition where $\xi \gtrsim \mathcal{O}(L)$. In view of the above considerations and the experimental results for the thermodynamic properties⁸ it came as a surprise to see that, even at and near T_λ , the new data for the rectangular capillaries with $L = 1 \mu\text{m}$ are indistinguishable from those for the cylinders⁹ with $r = 1 \mu\text{m}$ within combined experimental uncertainty.

On the basis of universality arguments one would expect the superfluid transition of bulk ^4He to belong to the same static universality class as the classical three-dimensional XY model of interacting spins. However, in the case of transport properties one must consider two subclasses; these are generally known as Model E and Model F of Halperin, Hohenberg, and Siggia.^{22,23} The dynamics of the superfluid transition belongs to Model F. Very recently, the resistivity as a function of the reduced temperature was calculated by Zhang *et al.*²⁴ for finite samples of a three-dimensional XY model using Monte Carlo and spin-dynamics simulations. The model used by these authors corresponds to Model E. Nonetheless the authors believe that their model should, to a good approximation, reproduce the dynamics of the superfluid transition. Their results for the *shape* of the resistivity of a quasi-two-dimensional geometry as a function of the reduced temperature are in agreement with our data. However, it should be noted that this comparison requires two scale parameters, one each for the temperature and the resistivity axis, to map

the XY model results onto the liquid helium case. These parameters determine the scale of the axes, but they do not affect the shape of the curve.

By virtue of the agreement with the cylinder data, our result for the value of the resistivity at T_λ also agrees well with the renormalization-group calculations by Töpler and Dohm²⁵ for capillaries of square cross-section, which had been seen before^{11,12} to agree with the measurements for cylinders.

In the next section, we describe briefly the experimental procedures and the data analysis and show that the heat currents employed to obtain the data used in the final analysis are small enough to avoid significant finite-power effects.¹⁰ In Sec. 3, we present the results of this work and compare them with available predictions based on simulation²⁴ or renormalization-group calculations.²⁵ A brief summary is provided in Sec. 4.

2. EXPERIMENTAL PROCEDURE

The apparatus was nearly identical to ones used previously.^{11,12} It contained two sample cells. One is shown in Fig. 2. It contained a specially produced GCA²⁶ of size $25 \times 25 \text{ mm}^2$ consisting of a central capillary area of approximately $20 \times 20 \text{ mm}^2$ surrounded by a solid glass border. The GCA was sealed with indium along the solid glass border to the copper top and bottom of the cell. The stainless-steel cell-wall had a much greater length than the GCA thickness in order to compensate for the different thermal contraction during cool down. This wall was bolted to the copper ends and provided mechanical support. The other cell was constructed similarly, but contained only a glass border and the area normally covered by the capillaries contained bulk helium. Each cell had a $5200 \text{ } \Omega$ resistive heater attached to its bottom. Measurements were made with various heater currents, ranging from $i_H = 1.54$ to $10 \text{ } \mu\text{A}$.

Figure 3 shows electron micrographs of the GCA. The capillaries, of $1 \times 10 \text{ } \mu\text{m}^2$ rectangular cross-section, are seen to be fairly uniform. The measured thickness of the GCA was $d = 0.92 \text{ mm}$.

The experimental measurement consisted of determining the temperature difference ΔT that developed in steady state when a heat current Q_{tot} was applied to the cell. For this purpose we used high-resolution susceptibility thermometers^{27,28} with a resolution of better than a nano-Kelvin. In Fig. 4, we show data for the resistance per unit length $R/d = \Delta T / (Q_{\text{tot}} d)$ for the four values $Q_{\text{tot}} = 12.3, 46.8, 83.2,$ and 520 nW . For $Q_{\text{tot}} \leq 83.2 \text{ nW}$ one sees that the results are independent of the applied power. For the largest $Q_{\text{tot}} = 520 \text{ nW}$ a significant power dependence appears. Figure 4 does not adequately show the behavior near T_λ where R/d becomes small. Thus, we show data for the same currents in this range in Fig. 5 on a

Finite-size Effects on the Thermal Resistivity of ^4He

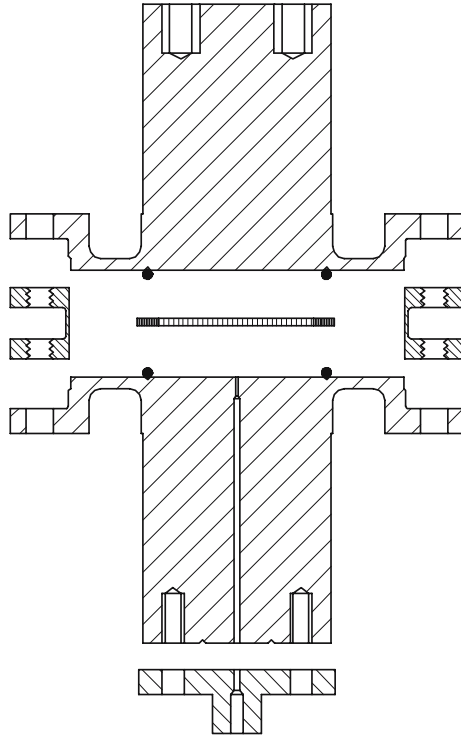


Fig. 2. Schematic diagram of the cell.

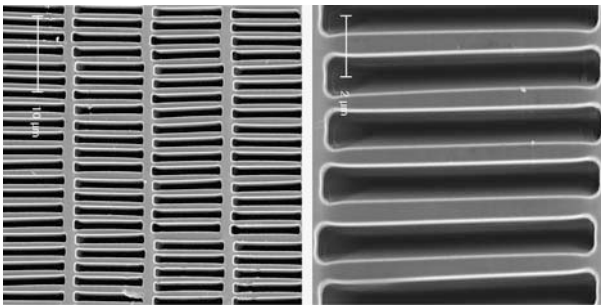


Fig. 3. Electron micrographs of the glass capillary array. The faint vertical bars correspond to 10 and $2\mu\text{m}$ in the left and right image respectively.

vertical logarithmic scale. Here even the data at the largest Q_{tot} do not deviate much from the other results. This is somewhat surprising because the usual “curvature” effect associated with the finite applied temperature

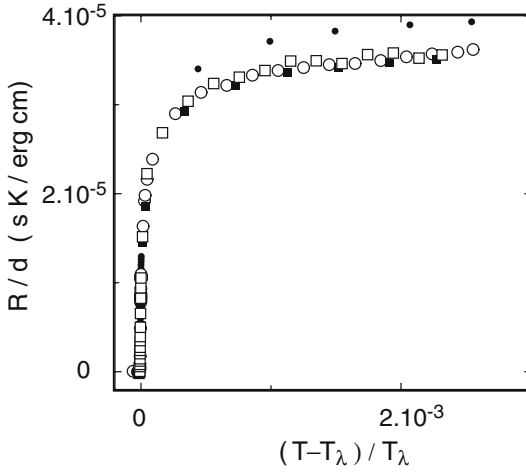


Fig. 4. Measurements of the resistance per unit length R/d as a function of the reduced temperature $t \equiv (T - T_\lambda)/T_\lambda$ with $Q_{\text{tot}} = 12.3$ (open squares), 46.8 (solid squares), 83.2 (open circles), and 520 (solid circles) nano-Watts.

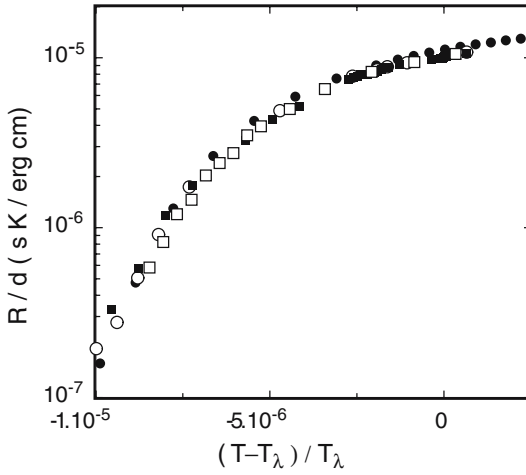


Fig. 5. Measurements of the resistance per unit length R/d , on a logarithmic scale, as a function of the reduced temperature t close to and below T_λ . The symbols are as in Fig. 4.

difference should be larger near and below T_λ than well above it.¹⁰ In any case, for further analysis we used only data for $Q_{\text{tot}} = 46.8$ and 83.2 nW. The smallest-power data were not used because the corresponding temperature differences were so small that significant random errors occurred.

Finite-size Effects on the Thermal Resistivity of ^4He

Similar measurements were made also for the bulk cell. The bulk data were used primarily to determine T_λ . Very close to T_λ a two-phase region appeared because of the influence of gravity on the transition.^{29,10} The transition temperature was taken in the middle of the two-phase region and, thusly defined, could be determined with a resolution of about 10^{-8} K.

A part Q of the total current Q_{tot} passed through the helium in the capillaries of thickness d and the remainder Q_0 passed through the cell wall and the glass which were also taken to be of effective thickness d . Assuming that the two currents correspond to two parallel conductors, we have

$$\frac{(Q + Q_0)d}{\Delta T} = \lambda(t)A + \lambda_0 A_0. \quad (1)$$

Here λ and A are the thermal conductivity and cross-sectional area of the helium in the capillaries, and λ_0 and A_0 are the effective thermal conductivity and cross-sectional area of the wall and glass. It is not practical to determine A and $\lambda_0 A_0$ independently. Instead the experimental data in the range $t > 1 \times 10^{-4}$, where finite-size effects are expected to be negligible, were fitted to Eq. (1), least-squares adjusting the two parameters A and $\lambda_0 A_0$ and using smoothed values of the conductivity $\lambda(t)$ of bulk helium.^{30,31} Such a fit is shown in Fig. 6 where the line is from Ref. 30. Parameters derived from these fits are listed in Table I. One sees that the different measurement sets at different powers gave consistent parameters, and that the values obtained are physically reasonable. Once A and $\lambda_0 A_0$

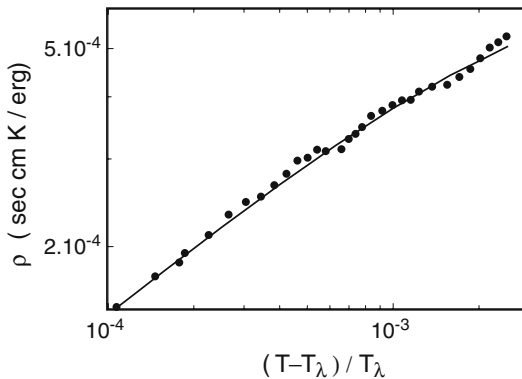


Fig. 6. The resistivity $\rho(t, L)$ as a function of t on logarithmic scales for $t > 10^{-4}$ where finite-size effects are negligible. Line: smoothed results from Ref. 30 for bulk helium. Circles: present measurements with parameters A and $\lambda_0 A_0$ derived from a fit of Eq. (1) to the data for $(Q + Q_0)/\Delta T$ using the bulk results for $\lambda(t, \infty) = 1/\rho(t, \infty)$ given by the line.

TABLE I

Parameters derived from a fit of Eq. (1) to the data for $(Q + Q_0)/\Delta T$ using the bulk results for $\lambda(t)$ given by the line in Fig. 6.

Sample	i_H $\mu\text{ A}$	Q_{tot} nW	$10^{-2}\lambda_0 A_0$ erg cm/s K	A cm^2
bulk	3	46.8	8.17	4.56
bulk	4	83.2	7.87	4.56
bulk	10	520.0	7.87	4.50
$1 \times 10 \mu\text{m}^2$	1.54	12.3	190	2.44
$1 \times 10 \mu\text{m}^2$	3	46.8	212	2.46
$1 \times 10 \mu\text{m}^2$	4	83.2	210	2.39
$1 \times 10 \mu\text{m}^2$	10	520.0	195	1.98

have been determined, one can obtain

$$\lambda(t, L) = \frac{(Q + Q_0)d}{A\Delta T} - \frac{\lambda_0 A_0}{A} \quad (2)$$

in the range $t < 10^{-4}$ where finite-size effects are significant.

3. RESULTS

In Fig. 7, we show results for the resistivity $\rho(t, L) = 1/\lambda(t, L)$ as a function of t on logarithmic scales for $t > 0$. For reference, the solid line shows the resistivity of bulk helium which vanishes as $t \rightarrow 0$. The new data for the $1 \times 10 \mu\text{m}^2$ capillaries are the solid circles. As t decreases well below $t \simeq 10^{-4}$, they fall above the bulk results, revealing the finite-size “rounding.” Surprisingly, they fall directly ontop of the open circles, which are the results from Ref. 11 for cylinders of radius $1 \mu\text{m}$. Also shown are the $r = 0.5 \mu\text{m}$ data from Ref. 11 They depart sooner from the bulk results and show more severe “rounding,” as is to be expected. All three sets of data for the finite geometries approach a constant value at $t \rightarrow 0$. This value will be discussed below and will be displayed in Fig. 10.

In Fig. 8, we show some of the results quite close to T_λ on linear scales (some data points near $t = 0$ were omitted for clarity). The vanishing of the bulk resistivity at T_λ is illustrated by the solid line. Some new data points for bulk helium and very close to T_λ are shown by the solid squares. Here too we see that the results for the rectangular geometry (solid circles) nearly coincide with the $r = 1 \mu\text{m}$ cylinder results (open circles). It is difficult to say whether the small difference that may exist near

Finite-size Effects on the Thermal Resistivity of ^4He

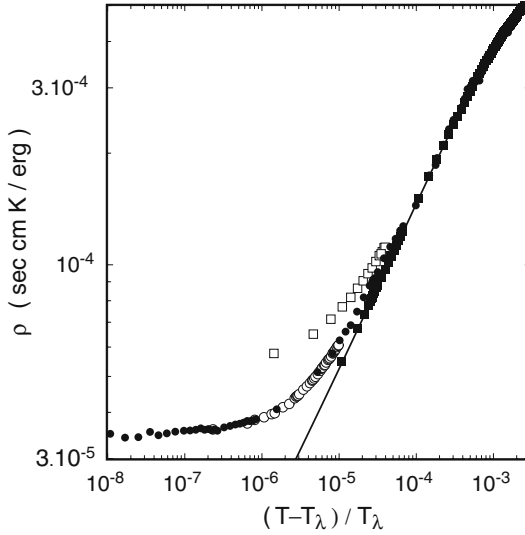


Fig. 7. The resistivity $\rho(t, L)$ or $\rho(t, r)$ as a function of the reduced temperature $t = T/T_\lambda - 1$ on logarithmic scales. Solid circles: present data for $(L=1) \times 10 \mu\text{m}^2$ GCA. Open circles: data from Ref. 11 for $r=1 \mu\text{m}$ cylindrical capillaries in a GCA. Open squares: data from Ref. 11 for $r=0.5 \mu\text{m}$ cylindrical capillaries in a GCA. Solid line: bulk helium results from Ref. 30. Solid squares: present data for bulk helium.

$t = -10^{-5}$ is a real effect or due to possible systematic errors in one data set or the other.

In Fig. 9, we compare our measurements for the $1 \times 10 \mu\text{m}^2$ capillaries with the simulations of Zhang *et al.*²⁴ In order to map the results for the classical XY model of spins onto the helium case, these authors introduced two multiplicative parameters, one each for the t -axis and the ρ -axis, which were adjusted so as to give the best possible agreement with our measurements. We note that this adjustment has no influence on the shape of the curve, and only changes the axis scales. As can be seen from Fig. 9, the agreement between simulation and experiment is quite good although there seem to be some systematic differences particularly at large t .

Finally, in Fig. 10, we compare the available experimental results for $\lambda(t=0, L) = 1/\rho(t=0, L)$ at the bulk transition with a renormalization-group (RG) calculation by Töpler and Dohm²⁵ which is shown as a dashed line (the solid line is a fit of a finite-size scaling prediction¹¹ to the measurements). The open square and circle are from Murphy *et al.*¹¹ for $r=0.5$ and $1 \mu\text{m}$, respectively. The plus is also from

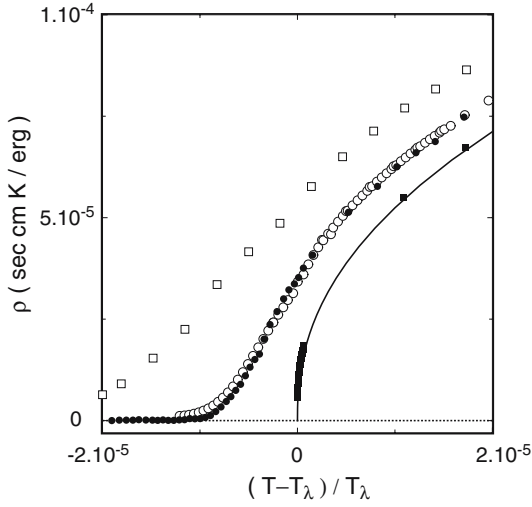


Fig. 8. The resistivity $\rho(t, L)$ or $\rho(t, r)$ as a function of the reduced temperature $t = T/T_\lambda - 1$ at small $|t|$ on linear scales. The symbols are as in Fig. 7. The dotted line is at $\rho = 0$.

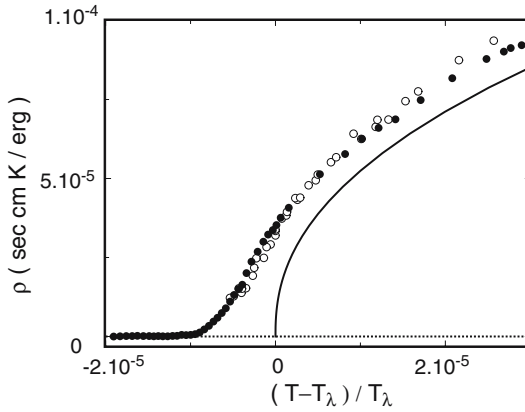


Fig. 9. The resistivity $\rho(t, L)$ as a function of the reduced temperature t at small $|t|$ on linear scales. Solid circles: this work for capillaries with a $(L = 1) \times 10 \mu\text{m}^2$ cross-section. Open circles: Monte Carlo and spin-dynamics simulations for a classical XY model. For the simulation the axes were scaled so as to achieve overall agreement with the experiment. The dotted line is at $\rho = 0$.

Finite-size Effects on the Thermal Resistivity of ^4He

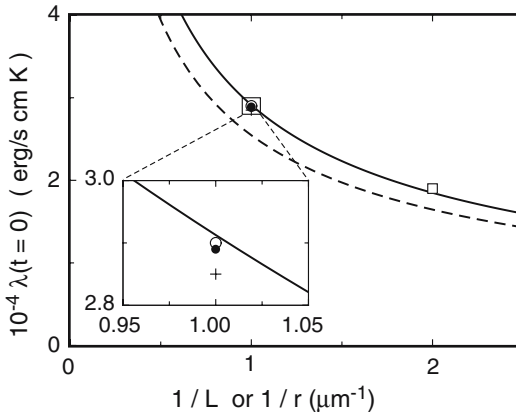


Fig. 10. The thermal conductivity at T_λ as a function of the inverse characteristic geometry size L for parallel plates or r for cylinders. The insert shows the data for $L = r = 1 \mu\text{m}$ in more detail. Open square: cylindrical capillaries with $r = 0.5 \mu\text{m}$ from Ref. 11. Open circle and plus: cylindrical capillaries with $r = 1 \mu\text{m}$ from Ref. 11. Solid circle: rectangular capillary of size $1 \times 10 \mu\text{m}^2$ ($L = 1 \mu\text{m}$) from this work.

those authors, from a separate experiment in a separate apparatus. The solid circle is our new result for capillaries with a $1 \times 10 \mu\text{m}^2$ cross-section. Again we see the remarkable agreement between the cylindrical and the parallel-plate geometry. The agreement with the RG calculation is quite good, considering the difficulties involved in calculating non-universal amplitudes.

4. SUMMARY

In this paper, we presented new measurements of the thermal resistivity $\rho(t, L)$ of liquid ^4He at saturated vapor pressure and near the bulk superfluid transition temperature T_λ . The fluid was confined in capillaries of nominal length 1 mm with a rectangular cross section of spacing $L = 1 \mu\text{m}$ and width $w = 10 \mu\text{m}$. Within our experimental uncertainty the results are indistinguishable from previous measurements for capillaries with a circular cross section of radius $r = 1 \mu\text{m}$. Equal results for the two systems are to be expected well away from the bulk transition where the correlation length is much smaller than the confining geometry because there surface effects are expected to dominate and the surface to volume ratio is equal. However, the equivalence persisted also at and near the transition where finite-size effects should dominate and where in principle different scaling functions could prevail. This behavior of a transport

property stands in contrast to that of thermodynamic properties⁸ which have dramatically different scaling functions for confinement in one, two, and three dimensions.

Our results are in reasonable agreement with the shape of $\rho(t, L)$ derived from Monte Carlo and spin dynamics simulations for the classical 3-dimensional XY model,²⁴ even though these simulations used a model that corresponds to Model E of Hohenberg and Halperin²² whereas the superfluid transition corresponds to Model F. However, the comparison between these simulations and the measurements for helium requires an adjustment of the scale of ρ and of t . Nonetheless, the agreement of the shape of $\rho(t, L)$ (albeit with small systematic differences particularly at large t), which is unaltered by the scale adjustment, is gratifying.

It had been noted earlier that there is good agreement between the resistivity measured at T_λ for capillaries with cylindrical cross-sections²⁰ on the one hand and RG calculations²⁵ for square cross-sections on the other. In view of the experimentally observed equivalence of the results for cylindrical and rectangular capillaries it thus comes as no surprise that our new data at T_λ also agree well with the theoretical calculation, even though the confinement geometry is different. We are not aware of RG calculations for a parallel-plate geometry. When such a calculation is done, it will be interesting to see whether the behavior near the transition is found to be the same or nearly the same as it is for the square cross-section.

ACKNOWLEDGMENTS

We are grateful to C. Zhang and D.P. Landau for providing numerical values for the results in Fig. 3 of Ref. 24, and to V. Dohm for several comments on a draft of this paper. The part of this work done at Santa Barbara was supported by NASA grants NAG3-2872 and NAG3-2903. The research described in this paper was partly carried out at the Jet Propulsion Laboratory, California Institute of Technology, under a contract with the National Aeronautics and Space Administration.

REFERENCES

1. For a general review of the role of the renormalization-group theory in statistical physics, see for instance M. E. Fisher, *Rev. Mod. Phys.* **70**, 653 (1998).
2. See, for instance, M. E. Fisher, in *Critical Phenomena*, Proceedings of the International School of Physics "Enrico Fermi" Course LI, M. S. Green (ed.), Academic, New York (1971).
3. See, for instance, M. N. Barber, in *Phase Transitions and Critical Phenomena*, C. Domb and J. L. Lebowitz (eds.), Academic, New York, vol. 8 (1983).
4. See, for instance, V. Privman, in *Finite Size Scaling and Numerical Simulations of Statistical Systems*, V. Privman (ed.), World Scientific, NJ (1990).

Finite-size Effects on the Thermal Resistivity of ^4He

5. For a review of the application of the theory of critical phenomena to the superfluid transition of liquid helium in finite geometries, see for instance, V. Dohm, *Phys. Script.* **T49**, 46 (1993).
6. M. Barmatz, I. Hahn, J. A. Lipa, and R. V. Duncan, *Rev. Mod. Phys.*, **79**, 1 (2007).
7. The universality of finite-size scaling for thermodynamic properties has been called into question recently by V. Dohm, *J. Phys. A: Math. Gen.* **39**, L259 (2006); and by X. S. Chen and V. Dohm, *Phys. Rev. E* **70**, 056136 (2004). [*Physica B* **329–333**, 202 (2003); *Phys. Rev. E* **67**, 056127 (2003); *Phys. Rev. E* **66**, 016102 (2002)].
8. M. O. Kimball, K. P. Mooney, and F. M. Gasparini, *Phys. Rev. Lett.* **92**, 115301 (2004).
9. A. Kahn and G. Ahlers, *Phys. Rev. Lett.* **74**, 944 (1995).
10. G. Ahlers, *J. Low Temp. Phys.* **115**, 143 (1999).
11. D. Murphy, E. Genio, G. Ahlers, F. C. Liu, and Y. Liu, *Phys. Rev. Lett.* **90**, 025301 (2003).
12. E. Genio, D. Murphy, G. Ahlers, F. -C. Liu, and Y. -M. Liu, *Adv. Space Res.* **35**, 87 (2005).
13. L. D. Landau, *J. Phys. USSR* **5**, 71 (1941) [English translation: *Collected Papers of L. D. Landau*, D. ter Haar (ed.), Gordon and Breach, NY (1965), p.301].
14. R. V. Duncan, G. Ahlers, and V. Steinberg, *Phys. Rev. Lett.* **58**, 377 (1987).
15. D. Frank and V. Dohm, *Phys. Rev. Lett.* **62**, 1864 (1989).
16. F. Zhong, J. Tuttle, and H. Meyer, *J. Low Temp. Phys.* **79**, 9 (1990).
17. R. V. Duncan and G. Ahlers, *Phys. Rev. B* **43**, 7707 (1991).
18. D. Frank and V. Dohm, *Z. Physik B* **84**, 443 (1991).
19. H. Fu, H. Baddar, K. Kuehn, and G. Ahlers, *Low Temp. Phys.* **24**, 69 (1998).
20. K. Kuehn, S. Mehta, H. Fu, E. Genio, D. Murphy, F. Liu, Y. Liu, and G. Ahlers, *Phys. Rev. Lett.* **88**, 095702 (2002).
21. L. S. Goldner and G. Ahlers, *Phys. Rev. B* **45**, 13129 (1992). [L. S. Goldner, N. Mulders, and G. Ahlers, *J. Low Temp. Phys.* **93**, 125 (1993)].
22. P. C. Hohenberg and B. I. Halperin, *Rev. Mod. Phys.* **49**, 435 (1977).
23. We are grateful to V. Dohm for reminding us of this.
24. C. Zhang, K. Nho, and D. P. Landau, *Phys. Rev. B* **73**, 174508 (2006).
25. M. Töpler and V. Dohm, *Physica B* **329–333**, 200 (2003).
26. The glass capillary array was produced for us by Hamamatsu Photonics K. K.
27. H. Fu, H. Baddar, K. Kuehn, M. Larson, N. Mulders, A. Schegolev, and G. Ahlers, *J. Low Temp. Phys.* **111**, 49 (1998).
28. B. J. Klemme, M. J. Adriaans, P. K. Day, D. A. Sergatskov, T. L. Aselage, and R. V. Duncan, *J. Low Temp. Phys.* **116**, 133 (1999).
29. G. Ahlers, *Phys. Rev.* **171**, 275 (1968).
30. W. Y. Tam and G. Ahlers, *Phys. Rev. B* **32**, 5932 (1985).
31. W. Y. Tam and G. Ahlers, *Phys. Rev. B* **33**, 183 (1986). [*Phys. Rev. B* **37**, 7898 (1988) (E)].